Journal of Sustainable Development of Energy, Water and Environment Systems

http://www.sdewes.org/jsdewes

Year 2027, Volume 15, Issue 1, 1140769

Original Research Article

Integrated Assessment of Photovoltaic Efficiency and Dynamic Line Rating for Curtailment Reduction in a 100 MW Solar Plant

Nuri Berisha, Enis Riza[*]
Power Engineering Department, University of Pristina, Pristina, Republic of Kosovo
e-mail: enis.riza@uni-pr.edu, nuri.berisha@uni-pr.edu

Cite as: Berisha, N., Riza, E., Integrated Assessment of Photovoltaic Efficiency and Dynamic Line Rating for Curtailment Reduction in a 100 MW Solar Plant, J.sustain. dev. energy water environ. syst., 15(1), 1140769, 2027,
DOI: https://doi.org/10.13044/j.sdewes.d14.0769

ABSTRACT

This paper links two aspects that are often studied separately: improving photovoltaic output through higher-efficiency photovoltaic modules and inverters, and increasing network transfer capability through dynamic line rating. The analysis considers a proposed 100 MW solar plant in Kuklibeg, Kosovo, and two 110 kV existing transmission lines for solar park connection, Line A and Line B. In Scenario 1, RETScreen is used to compare default photovoltaic modules with modules from default RETScreen product, Jinko Solar and Trina Solar under 95% and 98% inverter efficiencies. The best case is achieved with Jinko Solar and a 98% inverter, yielding 118,577 MWh/yr, 128,986 CO_2 t/yr avoided emissions, and reduced land use. Scenario 2 then evaluates whether this higher production can be integrated into the network using hourly static line rating and dynamic line rating on 15 July based on IEEE 738. While Line A can absorb the photovoltaic profile under both ratings, Line B experiences curtailment under static line rating and lower curtailment under dynamic line rating for the analysed case.

KEYWORDS

PV efficiency, Inverter efficiency, Dynamic line rating, Static line rating, Solar integration, Transmission capacity.

INTRODUCTION

As global environmental policies become increasingly strict, the urgency to address climate change has accelerated the global shift toward clean energy solutions [1]. In this context, renewable energy sources play a crucial role not only in sustainable energy production but also in reducing environmental impact. Optimizing all components involved in renewable energy systems, particularly those responsible for energy conversion, is essential. Such optimization contributes to higher energy output from the same installed capacity, reduced land usage, and lower CO_2 emissions [2].

One of the most critical components in renewable energy systems is the inverter, which converts direct current (DC) generated by photovoltaic (PV) panels into alternating current (AC) suitable for grid integration and consumption. Some research works have focused on increasing the efficiency of PV plants through the use of multilevel inverters (MLI). By employing a group of high-efficiency inverters, the output waveform approaches a pure sine wave, which in turn improves the overall efficiency of the energy produced by a PV plant [3]. In a similar way, though on a different topic, other studies, such as [4], have investigated the

[*] Corresponding author

use of FACTS devices to maximize the efficiency of power transfer from generation to consumption. While that work is more related to generator-based energy production, the main idea is similar: advanced power electronic devices can help increase system availability and deliver as much energy as possible to the end user.

In another study, the module inverter method was applied, where the topology consisted of a series resonant inverter, a high-frequency transformer, and a novel half-wave cycloconverter. Using this approach, an average efficiency of 95.9% was achieved, with the potential to exceed 96.5% [5]. Unlike works that develop models through multi-inverter or module-inverter configurations, this paper is focused on commercially available inverter catalogues, which already indicate efficiencies in the range of 95% to 98%. Therefore, the study is based on factory-produced inverters with integrated electronic devices, rather than proposing new inverter structures or topologies. On the other hand, PV efficiency and the method of installation also play a significant role in increasing the energy delivered to consumers. In this regard, [6] studied several factors affecting PV system production, such as temperature, series or parallel installation, tilt angle, and the use of different PV types, together with their impact on energy output. A similar study by [7] highlighted that using proper PV module brands, particularly newer ones, can improve the overall efficiency of the installed PV system.

Another important factor reviewed in this study is the reduction of CO_2 emissions through the installation of new renewable energy sources, specifically a 100 MW solar PV plant. In their work, emphasized the role of PV systems in achieving the EU Net Zero policy target of emission reduction [8]. Similarly, other studies highlighted that the use of PV systems instead of coal-based plants can significantly reduce emissions [9]. Another study concluded that by installing a 30 MW solar plant, CO_2 emission reductions can vary substantially over the lifetime of the PV system [10]. Likewise, emphasized that newly constructed centralized photovoltaic power stations can significantly reduce carbon dioxide emissions during their life cycle [11]. The same approach has been applied in this paper to analyse the CO_2 emission reduction potential of a 100 MW PV plant.

Of course, as discussed above, by increasing the efficiency of inverters or PV panels, the land requirements for installing large capacities and a significant number of panels can also be reduced. In their work, used a different approach than this paper, but with the same purpose of minimizing land use for PV panel installation [12]. They concluded that the median power density increased significantly for both fixed-tilt and tracking plants over time. While this paper focuses on improving PV panel efficiency to reduce land requirements, their study applied different strategies such as optimizing tilt angles and PV positioning. Similarly, analysed how site selection, system design, and installation methods can significantly affect land capacity utilization [13]. Furthermore, another study assessed the overall land required for PV deployment and emphasized that solar energy may occupy a noticeable share of total land at high penetration levels [14]. Therefore, exploring methods that reduce land use, even within limited premises, is a positive step toward facilitating the integration of large PV plants.

However, increasing generation efficiency alone does not guarantee that all produced energy can be delivered to the grid. For this reason, the transmission side must also be analysed together with the production side. In practice, overhead lines are usually operated using static line rating (SLR), where the allowable current is defined under conservative fixed weather assumptions. Although this approach ensures secure operation, it may underestimate the real transfer capability of the line during many operating hours. Dynamic line rating (DLR), on the other hand, determines the allowable current according to actual or time-varying weather conditions and the thermal condition of the conductor [15]. In most applications, this is done through the IEEE 738 heat balance, where joule heating and solar heat gain are balanced against convective and radiative cooling [16]. Because of this, DLR can provide a more realistic estimate of line capacity than SLR and is increasingly recognized as an important tool for renewable energy integration, congestion reduction, and curtailment mitigation [17]. This issue is directly relevant for photovoltaic plants, especially during peak summer production. Even if the PV plant is optimized through higher-efficiency modules and inverters, part of its output may still be curtailed if the transmission corridor cannot transfer the generated power during critical hours. For this reason, the present study does not stop only at the assessment of annual PV production. Instead, it links the production-side assessment with transmission-side flexibility. In Scenario 1, RETScreen-based results are used to compare different PV module options and inverter efficiencies for the proposed 100 MW solar plant in Kuklibeg, Kosovo. After identifying the best production case, Scenario 2 evaluates whether this higher output can actually be integrated into the network through two existing 110 kV lines, referred to as Line A and Line B. For this purpose, hourly SLR and DLR values are analysed for the critical summer day of 15 July using conductor and weather data together with the IEEE 738 thermal balance approach [16]. In this way, the paper connects the best production case from Scenario 1 with the real transmission capability assessment of Scenario 2. In addition, previous studies have shown that DLR can reveal additional transfer capability compared to SLR and can support the integration of variable renewable generation by reducing unnecessary congestion and curtailment [18].

The selected proposed location for the study is Kuklibeg, Kosovo, which was chosen because of its high potential for solar photovoltaic installations. According to solar radiation zoning maps of Kosovo, this area receives some of the highest solar irradiance in the country, making it an ideal candidate for feasibility analysis and renewable energy integration [19]. According to Kosovo's energy strategy, the integration of renewable energy is one of the most important steps toward achieving the goals of renewable energy technology integration into the grid [20]. Increasing the share of carbon-free electricity generation, such as the proposed project, will provide benefits not only for future research on energy production, but also for the environmental and social development of the country.

The purpose of this study is to show that inverter efficiency and PV module selection should not be evaluated only from the production point of view, but also from the transmission point of view. Even though inverter efficiency may appear as a small technical detail, its impact on annual energy production, avoided CO_2 emissions, and land use can be significant. At the same time, the additional production achieved in Scenario 1 can only be fully utilized if the network can transfer that power without unnecessary curtailment. Therefore, the combined assessment of PV efficiency and line rating provides a more realistic picture of renewable energy integration.

This study aims to provide an accurate feasibility assessment of selecting appropriate equipment to optimize both energy output and environmental performance, while also evaluating whether the existing transmission system can accommodate that energy under static and dynamic rating conditions. Its main contribution lies in the combined analysis of inverter efficiency, PV module selection, CO_2 emission reduction, land use efficiency, and transmission transfer capability through SLR and DLR. In this way, the paper offers a more complete perspective for future renewable energy planning and policy development, especially in systems where renewable generation growth must be supported by more flexible use of existing transmission infrastructure.

LITERATURE REVIEW

Recent literature shows that PV efficiency improvement is no longer discussed only at cell level, but increasingly at plant level, where module selection, inverter behaviour and system optimization are treated together. Zhang *et al.* reviewed intelligent optimization methods for PV inverter systems and showed that inverter control quality directly affects conversion performance, grid compatibility and operational stability in modern PV plants [21]. Lim *et al.* further demonstrated that inverter efficiency degradation can be identified from operating data and that even relatively small efficiency losses become relevant in long-term energy delivery [22]. Bahloul and Khadem also showed that utility-scale PV performance is sensitive to inverter loading ratio design, meaning that the AC energy finally exported to the grid depends not only on

DC module efficiency but also on how the DC/AC conversion stage is dimensioned and operated [23]. These studies support the first scenario of this paper, where higher-efficiency PV modules and inverters are evaluated as interacting determinants of annual AC energy output.

Broader post-2023 review papers confirm that PV performance gains are being driven by both improved module technologies and system-level optimization. Ali *et al.* summarized recent advances in photovoltaic technology and highlighted that new cell architectures, better materials and improved integration concepts continue to increase solar conversion efficiency [24]. Likewise, Iturralde Carrera *et al.* showed that current optimization trends in photovoltaic systems increasingly combine design optimization, control, forecasting and energy management methods to maximize yield under real operating conditions [25]. For utility-scale projects such as Kuklibeg, this means that improvements in module and inverter efficiency can be interpreted as practical pathways for higher annual production, lower specific land use and greater CO_2 mitigation per installed megawatt. For transmission integration, the DLR literature consistently shows that the thermal capability of overhead lines is weather-dependent and is often significantly higher than the conservative value assumed under static line rating. Another study [26] analysed the enabling technologies behind DLR, while IEEE Std 738-2012 and the CIGRE thermal rating guide provide the methodological basis for conductor heat-balance calculations under changing weather conditions [27]. Michiorri *et al.* addressed forecasting aspects [28], Douglass and Edris validated DLR through field studies [29], and Matus *et al.* highlighted the importance of critical-span identification [38]. Further work has shown the practical value of DLR for increasing distributed generation hosting capacity and for selecting suitable DLR systems in real power networks [30]. Karimi *et al.* synthesized the broader state of the art [15], while Ringelband *et al.* and Seppa linked dynamic line monitoring with renewable-grid integration and real-time transmission capacity enhancement [31]. Together, these studies justify the integrated framework used in this paper: once Scenario 1 increases PV production, Scenario 2 evaluates whether the additional power can actually be transferred by Line A and Line B under DLR and SLR assumptions.

Previous studies mainly treated PV efficiency improvement and line transfer capability as separate topics. PV-related studies focused on better inverters, modules, and emissions, while DLR studies focused on increasing overhead line capacity under real weather conditions. The missing part in the literature is the direct link between these two sides. This paper fills that gap by first identifying the best PV production case and then checking, through SLR and IEEE 738-based DLR, whether that higher generation can actually be transferred through the existing 110 kV network without curtailment.

Table 1 presents the identified research gaps in tabular form, including the main focus of each reference, the work performed by previous studies, the corresponding research gap, and the contribution of the present paper.

Table 1. Research GAP.

Ref.	Focus	What they did	Gap	This paper
[3]	Inverter efficiency	Improved PV efficiency through multilevel inverter topology.	No practical utility-scale comparison; no grid link.	Compares practical inverter efficiencies in a 100 MW PV plant.
[7]	PV module efficiency	Showed that better PV modules increase energy output.	Did not combine module choice with inverter efficiency and grid limits.	Compares module options together with inverter efficiency.
[10]	CO_2 reduction	Evaluated emission reduction from solar PV projects.	Did not link emissions with equipment efficiency and transmission capability.	Assesses avoided CO_2 for the best PV case and its grid integration.
[15]	DLR/SLR	Reviewed dynamic thermal rating of overhead lines.	No link with PV production optimization.	Links PV efficiency results with hourly line rating analysis.
[17]	DLR/SLR	Studied dynamic rating management under varying weather.	Focused only on line operation.	Combines line rating with PV yield, land use, and CO_2 analysis.

Mathematical Model

One of the methods used in this case study to achieve reliable results was the mathematical approach, where formulas for the efficiency of PV arrays, inverters, and the energy produced by solar power were applied, based on the RETScreen textbook analysis [32]. The formula for the efficiency of a PV array is given below [33]:

$$\eta_p = \eta_r[1 - \beta_p(T_c - T_r)] \quad (1)$$

where: η_p is PV module efficiency at operating conditions (%), η_r is PV module efficiency at the reference temperature (%), β_p is temperature coefficient of module efficiency (°C^{-1}), T_c is PV cell temperature (°C) given by RETScreen database, and T_r is reference cell temperature (25 °C). According to the formulas and tables calculated the highest value of T_c is reached in the Mono-Si PV system.

Our proposed model is an on-grid system, and the suggested inverters with different efficiencies are assumed to be equal to the nominal array power. The energy available to the grid is the energy produced by the array, reduced by the inverter losses, as given in:

$$E_{grid} = E_a \times \eta_{inv} \quad (2)$$

where: E_{grid} is the energy delivered to the grid from the proposed PV plant, E_a is the energy produced by the PV plant from the source, and η_{inv} is the inverter efficiency.

In reality, not all of the sourced energy can be injected into or absorbed by the grid, as it depends on the grid configuration and the capability of the PV array to capture energy from the source. Hence, the actual amount of energy delivered to the grid is given by:

$$E_{deliv} = E_{grid} \times \eta_{abs} \quad (3)$$

where: E_{deliv} is the real power sent to grid by the new system, E_{grid} is the power that can be sent to grid from the system in their maximum conditions and η_{abs} is the absorption efficiency of PV arrays.

Another important equation that has been used for energy production scenarios is inverter efficiency, which is calculated from:

$$\eta_{inv} = \frac{P_{out}}{P_{in}} \quad (4)$$

where: η_{inv} is the efficiency of inverter, P_{out} is energy delivered to the load as AC power and P_{in} is the power given from the source to the PV plan as DC power.

What is very important are the inverter losses, which determine the efficiency differences between inverters from different manufacturers. The lower the losses, the higher the inverter efficiency, and consequently, the greater the amount of energy delivered to the load. The formula for inverter losses is given as:

$$P_{loss} = P_0 + k \times P_{out} \quad (5)$$

where: P_{loss} are inverter losses, P_0 are constant losses, P_{out} is power delivered to the load and k is the coefficient of losses based on type of inverter.

One important relation between PV module efficiency and solar irradiance is the land area required, which can be expressed as:

$$A = \frac{P}{G \times \eta_{pv}} \quad (6)$$

where: A is land area required (m²), P is installed PV capacity (W), G is solar irradiance (W/m²), η_{pv} is PV module efficiency.

These parameters enabled a detailed scenario-based analysis to assess the benefits of high efficiency inverters in improving energy yield, reducing land footprint, and lowering greenhouse gas emissions.

The thermal rating of the overhead line was determined using the IEEE 738 heat balance approach [16]. The transferable power capacities were determined using the input data and the formulas presented below:

$$q_c + q_r = q_s + q_j \tag{7}$$

where: q_s is Solar Heat Gain, q_r is Radiative Heat Loss, q_c is Convective Heat Loss, and q_j is Joule Heating.

Solar Heat Gain is given with the below formula:

$$q_s = \alpha \times Q_{se} \times D \tag{8}$$

where: α is soar absorptivity and in our case is 0.5, Q_{se} is total solar radiation (W/m^2) and is taken from weather data, and D is the diameter of the conductor from the conductor datasheet.

Radiative Heat Loss is given with the below formula:

$$q_r = \pi \times D \times \varepsilon \times \sigma \times [(\frac{T_c + 273}{100})^4 - (\frac{T_a + 273}{100})^4] \tag{9}$$

where: D is the diameter of the conductor from the conductor datasheet, ε is emissivity, σ is Stefan-Boltzmann constant 5.67×10^{-8} W/(m^{2}K^4), T_c is the conductor temperature at 75 °C, and T_a is the ambient temperature from the weather data.

For formal IEEE 738-based analysis, the full natural and forced convection equations should be used.

$$q_c = K_a \times [1.01 + 1.35 \times Re^{0.52}] \times K_f \times (T_c - T_a) \tag{10}$$

$$Re = \frac{D \times \rho \times V}{\mu_f} \tag{11}$$

where: K_a is wind direction factor, λ is thermal conductivity = 0.0271 W/(m·K), ρ is air density = 1.127 kg/m³, T_c is conductor temperature, T_a is ambient temperature, D is conductor diameter and V is wind speed, Re is the Reynolds number, k_f is the thermal conductivity of air, and μ_f is the dynamic viscosity of air.

For the analysed transmission lines, K_a has been calculated for each hour, k_f = 0.0271 W/(m·K) and μ_f = 1.9 × 10^{-5} kg/(m·s). A wind-angle correction factor of 0.6 was adopted in the DLR calculations to account for non-perpendicular wind conditions. The exact line azimuth and span-specific meteorological exposure were not available and are considered a limitation of the present study.

And finally, I_{DLR} is calculated as below:

$$I_{DLR} = \sqrt{\frac{q_c + q_r - q_s}{R(T_c)}} \tag{12}$$

where $R(T_c)$ is the conductor AC resistance at the operating conductor temperature T_c. In this study, $R(T_c)$ corresponds to the conductor resistance at 75 °C and is taken as 0.14 Ω/km.

The transferred power under DLR conditions was then calculated using the following formula:

$$P = \sqrt{3} \times U \times I_{\mathrm{DLR}} \tag{13}$$

where: U is the nominal voltage of the transmission lines and I_{DLR} is the calculated current derived by IEEE 738 formulas.

The wind-angle correction factor K_{angle}, was calculated according to the IEEE 738 formulation by using the hourly wind direction from the NASA POWER dataset and the representative conductor azimuth of the studied corridor:

$$K_{angle} = 1.194 - cos\Phi + 0.194\cos(2\Phi) + 0.368\sin(2\Phi) \tag{14}$$

where: ϕ is the acute angle of incidence between the direction of the wind flow and the longitudinal axis of the conductor.

The conductor axis was taken as 268.1°/88.1° for the existing lines corridor. For each hour, the acute angle between the wind direction and the conductor axis was calculated and then used to determine the corresponding hourly. In this study, the calculated hourly K_{angle} values ranged from 0.881 to 0.993.

CASE STUDY 1

Improved Photovoltaic Production Through Higher Module and Inverter Efficiency

The case study of this paper is a proposed 100 MW PV Plant in Kuklibeg, a village in the Dragash municipality of Kosovo. The proposed location was chosen due to its high potential for PV installation according to the solar mapping zone of Kosovo. As can be seen from the map in the Figure 1, the study area has a high potential, and from an environmental perspective, there are many places far from residential areas, making it possible to achieve energy production with minimal environmental and social impact.

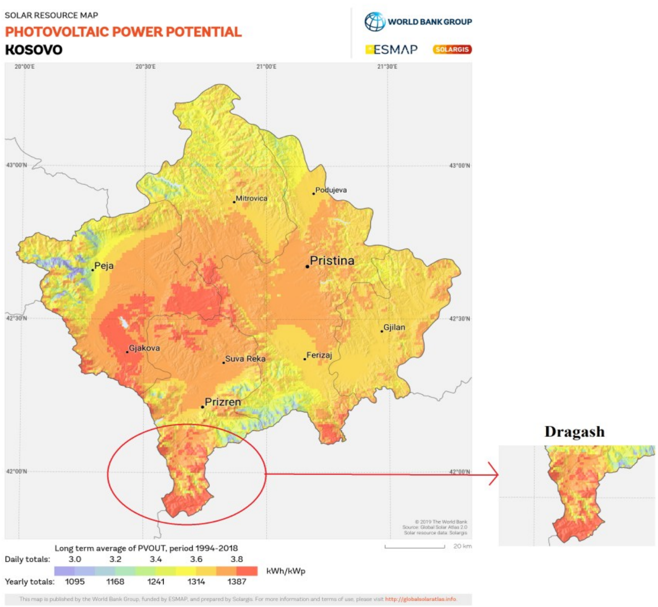

Figure 1. Solar mapping zone of Kosovo [19].

This case study focuses only on energy production scenarios based on different inverter efficiencies and different PV brands with varying efficiencies. It does not consider other aspects such as costs and transmission integration, because in Dragash there is still no transmission grid. However, in the future, based on the Transmission Development Plan, new 110 kV transmission assets are expected to be installed [34].

Another aspect that could be considered in the future is the social impact, is on social cohesion in Kosovo regarding the creation of new jobs. This project could also generate new job opportunities for the citizens of Dragash.

In RETScreen, as can be seen in **Figure 2** below, the geographic location selected was Kuklibeg, Kosovo. The climate database embedded in RETScreen was used to extract meteorological conditions, including solar irradiance, ambient temperature, and precipitation for the site [32].

Figure 2. Geographic location selection in RETScreen [32].

As it can be seen from **Figure 3**, the daily solar radiation at the selected location is relatively high, especially during the months from April to August, where values exceed 6 kWh/m²/day, peaking around 7 kWh/m²/day in July. This clearly indicates that the site has excellent solar potential and is suitable for photovoltaic installation throughout the year. The average annual solar radiation remains consistently favourable for energy production [33].

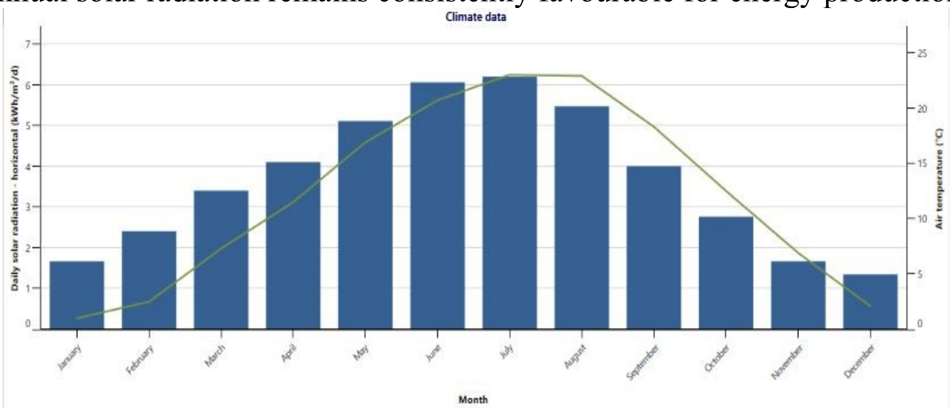

Figure 3. Daily solar radiation at the selected location [32].

According to RETScreen data, the climate data used in the analysis, including daily solar radiation and air temperature, are sourced from NASA's satellite database and other data from similar papers. This adds a level of credibility and accuracy to the resource assessment, ensuring that the PV project is based on reliable and globally recognized datasets.

In the **Table 2** below are presented some of the parameters taken directly from the RETScreen database [32].

Table 2. Panel producer parameters.

	Jinko Solar	Trina Solar
Solar Tracking mode	Fixed	Fixed
Slope	42°	42°
Azimuth	0°	0°
PV Type	mono-SI	mono-SI
Capacity per unit	615 W	630 W
Number of units	162750	150450
PV Efficiency	22%	21.40%
Nominal Operating Cell temperature	45 °C	45 °C
Temperature coefficient	0.40%	0.40%
Solar collector area	454960 m²	467520 m²

The main objective was to assess how inverter efficiency and module performance impact the total electricity exported to the grid, with a focus on maximizing energy yield and minimizing CO_2 emissions.

Table 3 shows the results of the comparative analysis results of the annual energy output from a 100 MW photovoltaic system, based on different combinations of inverter technologies, traditional and high efficiency, and PV panel manufacturers as: Default, Jinko Solar, and Trina Solar.

Table 3. Annual Energy Output for six different scenarios.

Scenario	Inverter Efficiency	PV Panel Producer	Annual Energy Output (MWh)
1	0.95	Default	114843
2	0.98	Default	118469
3	0.95	Jinko Solar	114947
4	0.98	Jinko Solar	118577
5	0.95	Trina Solar	114899
6	0.98	Trina Solar	118528

The first scenario analysed was the default setup using average system parameters. With a traditional inverter efficiency of 0.95, the system produced 114,843 MWh annually. When the same system was simulated with a high efficiency inverter at 0.98 efficiency, the output increased to 118,469 MWh, an improvement of approximately 3,626 MWh or 3.16%. This gain demonstrates the direct benefit of using high efficiency inverters, especially in large scale systems.

Subsequently, two manufacturers, Jinko Solar and Trina Solar, were assessed under 0.98 inverter efficiency scenarios, but now, with Panel efficiency impact on the energy production and land use for the proposed installed 100 MW, as in the table below:

For Jinko Solar, the energy output was 114,947 MWh with traditional inverters and increased to 118,577 MWh using high efficiency inverters, resulting in a gain of 3,580 MWh. Similarly, for Trina Solar, the output rise from 114,899 MWh with a traditional inverter to 118,528 MWh with a high efficiency inverter, leading to an increase of approximately 3,628 MWh annually, and calculations are positive.

These results consistently show that regardless of panel manufacturer, improving inverter efficiency from 95% to 98% leads to a noticeable increase in total energy production. Given similar capital investment, this directly translates to a lower cost per MWh generated, reduced emissions per energy unit, and more efficient land use.

In conclusion, the findings strongly support the adoption of modern high-efficiency inverter technologies in large-scale PV projects in Kosovo and beyond, as they offer measurable energy and environmental benefits.

In **Figure 4**, the comparative results are presented graphically, illustrating the annual energy output for each PV configuration using both traditional and modern inverters. The chart clearly highlights the performance improvement achieved with high-efficiency inverters across all panel types.

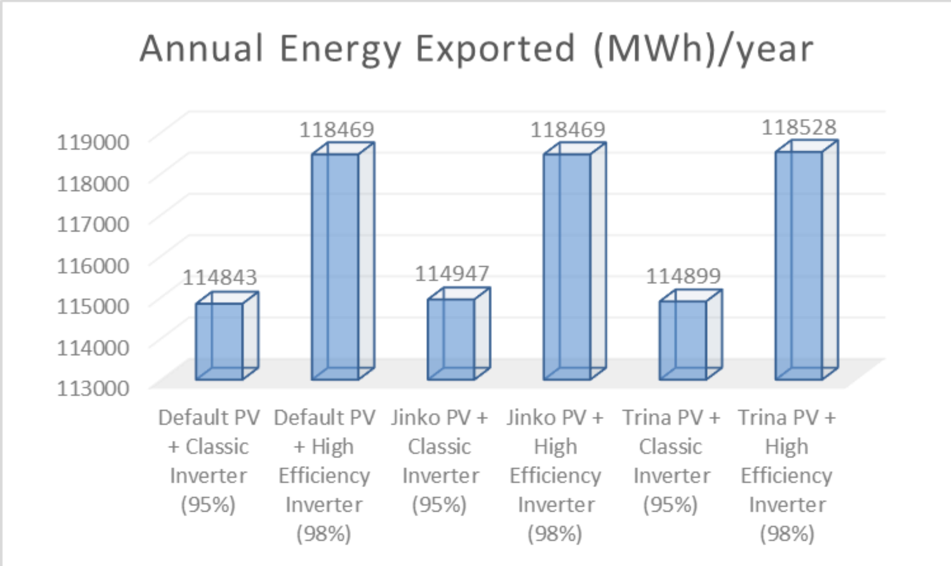

Figure 4. Annual energy output for each PV configuration.

As illustrated in **Figure 5**, a clear comparison is made between the use of traditional inverters with efficiency of 0.95 and modern inverters with efficiency of 0.98 in terms of CO_2 emission reduction. According to RETScreen's emission analysis, the system equipped with traditional inverters results in a gross annual GHG emission reduction of 124,923 t CO_2, while the use of high-efficiency inverters increases this reduction to 128,986 t CO_2. This difference confirms that even a small increase in inverter efficiency directly contributes to greater mitigation of greenhouse gas emissions. Therefore, improving inverter efficiency, even by a few percent, plays a significant role in reducing the environmental impact of large-scale PV systems.

In this part of the study, a detailed emission analysis was performed using RETScreen to evaluate the potential CO_2 emission reduction for six different photovoltaic system configurations. Each scenario was simulated by varying two parameters: the type of inverter used, traditional with 95% efficiency and modern with 98% efficiency, and the photovoltaic panel manufacturer: Default RETScreen, Jinko Solar, and Trina Solar. For each case, the annual energy exported to the grid was entered into the emissions module to determine the gross annual GHG (CO_2) reduction compared to a baseline scenario. The results are summarized in **Table 4**. As shown, the use of high-efficiency inverters consistently results in higher CO_2 reductions than traditional inverters. For instance, the combination of Jinko panels with a high-efficiency inverter achieves the highest reduction, with 128,986 t CO_2 annually. Even small differences in inverter efficiency, when scaled to a 100 MW plant, show significant environmental impact. Across all configurations, the modern inverter outperforms its traditional counterpart by reducing an additional 3,800–4,100 tonnes of CO_2 annually, depending on the panel used.

In the **Table 4** are presented the evaluation of the potential CO_2 emission reduction for six different photovoltaic system configurations. The CO_2 reduction values were calculated automatically by RETScreen based on the location-specific grid emission factor available in the RETScreen database.

Table 4. CO2 emission reduction for six scenarios.

Scenario	Inverter Efficiency	PV Panel Producer	CO_2 Reduction (t CO_2/yr)
1	0.95	Default	124923
2	0.98	Default	128868
3	0.95	Jinko Solar	125037
4	0.98	Jinko Solar	128986
5	0.95	Trina Solar	124985
6	0.98	Trina Solar	128932

These values clearly demonstrate the positive environmental impact of adopting higher efficiency inverters, not only by increasing total energy output but also by significantly reducing greenhouse gas emissions. While the choice of panel manufacturer also affects the total energy output due to slight variations in efficiency and design, the inverter type shows a more consistent and measurable influence on emission reduction. To visually support this analysis, the table above is also illustrated in **Figure 5**, providing a comparative view of all six scenarios with their respective CO_2 reduction values.

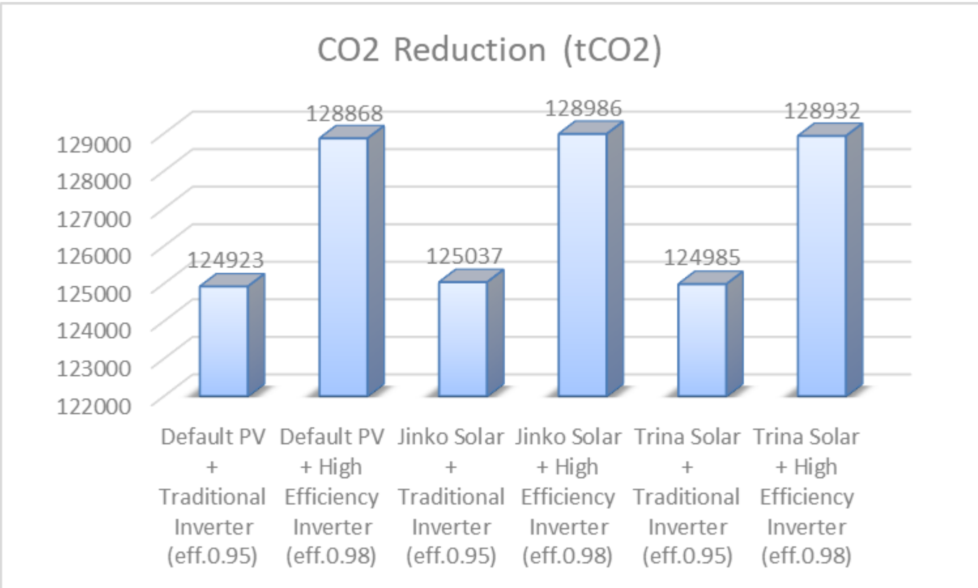

Figure 5. CO2 emission reduction.

Land use optimization is one of the most important aspects to be considered in all renewable energy projects, as it allows for maximizing system performance while minimizing land requirements. Selecting a PV panel brand with higher efficiency can significantly reduce the land needed for installation, while still achieving the same, or even higher energy output.

Three PV module configurations available in the RETScreen database were evaluated: the default RETScreen PV module (15.75%), Jinko Solar (22%), and Trina Solar (21.4%). Jinko Solar and Trina Solar were selected as representative commercially available high-efficiency PV modules included in the RETScreen database, while the default RETScreen module was used as a reference case for comparison. The land use values reported in **Table 5** represent the total photovoltaic plant area estimated by RETScreen for the specified installed capacity and module characteristics. The calculations were performed using the default RETScreen methodology and assumptions.

Table 5 Land use saving of three scenarios.

Scenario	PV Panel Efficiency	PV Panel Producer	Annual Energy Output [MWh]	Land use [m^2]
1	15.75%	Default	114843	634921
2	22%	Jinko Solar	114947	454960
3	21.4%	Trina Solar	114899	467520

The **Figure 6** below presents the analytical graphs and trends demonstrating how land use can be reduced by utilizing PV panels with higher efficiency. It can be observed that, for the same installed power capacity, the required land area can be reduced significantly. For example, the difference in land use between the Jinko Solar and Trina Solar PV modules amounts to 12,560 m², which is a considerable saving, particularly important for countries with limited land resources.

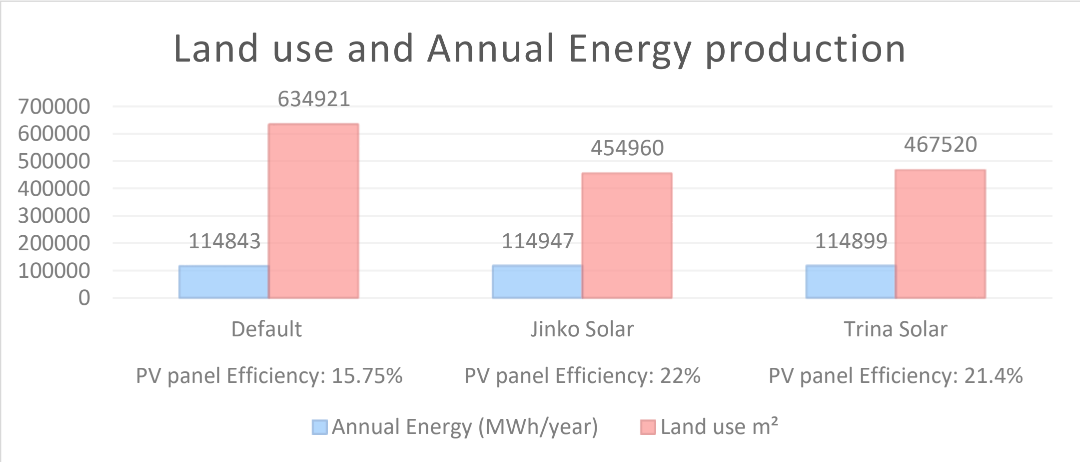

Figure 6. Land use saving.

All emission calculations were performed using the RETScreen database. The emission factor was automatically assigned by the software for the selected location, as shown in the while the transmission and distribution losses were based on the annual reports published by the Energy Regulatory Office of Kosovo **[35]**.

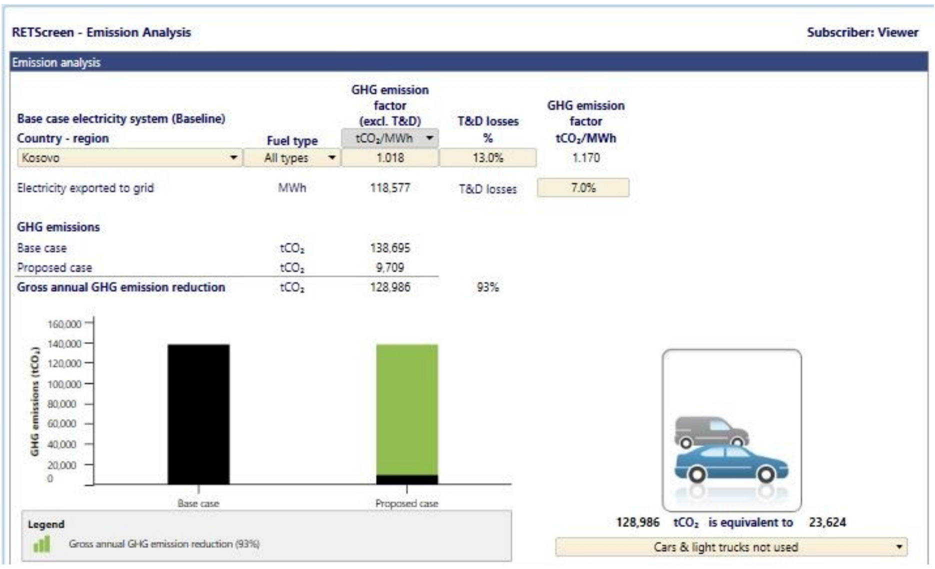

Figure 7. Emission factor used for CO2 emission reduction.

CASE STUDY 2

Transmission of the Increased Photovoltaic Output Using Static Line Rating and Dynamic Line Rating

After identifying the most favourable production case, the second scenario examines whether the transmission network can absorb the increased power. The uploaded daily solar profile was added hour by hour to the existing hourly load of the two representative 110 kV corridors, denoted in this paper as Line A and Line B. In this way, the total export profile for each corridor (existing line load plus PV production) was first checked against the conservative SLR limit and then against the hour-by-hour DLR capability derived from the same ACSR 240/40 mm² conductor data for both lines. The hourly PV production profile and the existing hourly load used for Line A and Line B is presented in the **Table 6** below.

Table 6. The hourly PV production profile and the existing hourly load used for Line A and Line B.

PV Production		Line A		Line B	
Time	MW	Time	MW	Time	MW
0	0.00	0	17.21	0	33.62
1	0.00	1	15.83	1	24.80
2	0.00	2	12.85	2	21.64
3	0.00	3	12.00	3	19.99
4	0.00	4	11.35	4	18.29
5	0.00	5	11.85	5	20.26
6	0.20	6	11.15	6	22.65
7	10.05	7	12.40	7	34.67
8	37.07	8	14.01	8	45.71
9	63.77	9	18.81	9	53.72
10	80.76	10	21.17	10	59.73
11	91.16	11	20.17	11	62.32
12	93.77	12	20.71	12	60.85
13	92.80	13	22.23	13	54.90
14	88.04	14	24.66	14	52.68
15	76.06	15	24.64	15	52.36
16	56.38	16	25.97	16	50.68
17	27.47	17	25.98	17	50.76
18	3.46	18	29.00	18	47.54
19	0.00	19	25.94	19	45.98
20	0.00	20	21.79	20	42.56
21	0.00	21	22.90	21	40.05
22	0.00	22	23.27	22	36.32
23	0.00	23	19.95	23	38.94

The hourly loading values of Line A and Line B represent measured power flows on the analysed transmission corridors obtained from KOSTT operational data. For publication clarity, both analysed corridors are referred to as Line A and Line B, where these corridors represent actual existing 110 kV transmission lines that were selected because of their potential relevance for future renewable energy integration and because the terrain characteristics and meteorological conditions along their routes are similar to those of the proposed photovoltaic plant site.

The two analysed lines, referred to as Line A and Line B, are existing 110 kV corridors in the Kosovo transmission network. Each line connects two different substations and forms part of the interconnected transmission system. The measured power-flow direction on the analysed critical day is illustrated in the **Figure 8** below.

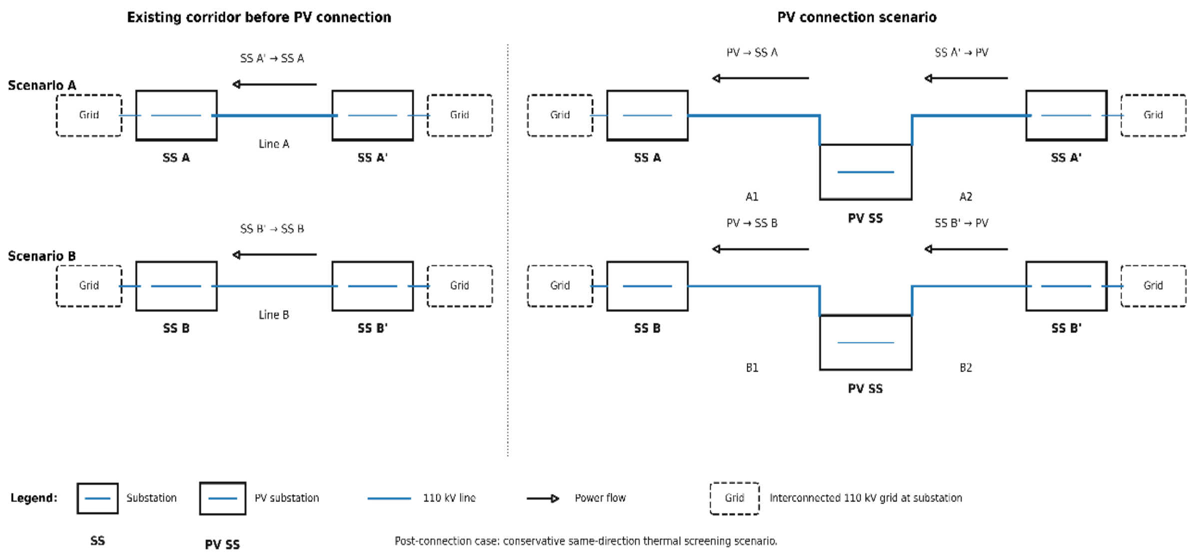

Figure 8. Critical day of same direction scenario for PV integration in a 110 kV network.

For the pre-feasibility assessment, a conservative same-direction operating case was considered. In this case, the pre-existing power flow on each original corridor is assumed to continue toward the newly introduced PV substation after the line is cut and connected to the PV substation busbars. At the PV substation, the incoming transfer component and the PV generation are assumed to contribute in the same direction and are transported through the other cut section toward the corresponding substation

The same existing conductor data were applied to both lines, namely an ACSR 240/40 mm² conductor at 110 kV taken at KOSTT. **Table 7** summarizes the common electrical and thermal parameters used in the IEEE 738 calculations.

Table 7. Existing line and conductor data used for the IEEE 738 evaluation in Case 2.

Item	Symbol	Value used in Case 2
Line names used in the paper	-	Line A and Line B
Voltage level	U	110 kV
Conductor type	-	ACSR 240/40 mm²
Outer diameter	D	21.4 mm
DC resistance at 25°C	$R25$	0.12 Ω/km
DC resistance at 75°C	$R75$	0.14 Ω/km
Maximum conductor temperature	$T_{c,max}$	75 °C
Emissivity	ε	0.5
Solar absorptivity	α	0.5

To make the hourly procedure transparent, **Table 8** reports the ambient temperature, wind speed, wind direction and solar radiation values that were used as inputs to the DLR model for both existing lines. Hourly meteorological data were obtained from NASA POWER for 15 July 2025 in UTC time at latitude 42.2794° and longitude 20.9031°, with an average MERRA-2 elevation of 665.3 m. The extracted parameters were T2M, WS10M, WD10M, and

ALLSKY_SFC_SW_DWN, representing air temperature at 2 m, wind speed at 10 m, wind direction at 10 m, and all-sky surface shortwave downward irradiance, respectively.

Table 8. Hourly meteorological input data used for the DLR calculation on 15 July 2025.

YEAR	MO	DY	HR	T2M	WS10M	WD10M	ALLSKY_SFC_SW_DWN
2025	7	15	0	20.78	2.34	7.6	0
2025	7	15	1	20.42	2.4	6	0
2025	7	15	2	20.33	2.43	3.8	0
2025	7	15	3	20.57	2.6	359.6	12.55
2025	7	15	4	21.75	3.32	356.5	92.72
2025	7	15	5	23.44	4.42	14.9	199.85
2025	7	15	6	24.95	5.12	28.1	329.6
2025	7	15	7	25.71	4.84	30.8	409.4
2025	7	15	8	26.18	4.41	30.8	512.1
2025	7	15	9	26.61	4.07	28	592.42
2025	7	15	10	26.99	3.77	23.1	655.42
2025	7	15	11	27.44	3.56	18.8	741.12
2025	7	15	12	27.9	3.45	18.7	662.83
2025	7	15	13	28.47	3.34	22.5	607.97
2025	7	15	14	29.04	3.33	26	442.33
2025	7	15	15	29.06	3.43	29.5	270.48
2025	7	15	16	28.29	3.5	32.7	142.9
2025	7	15	17	25.89	2.29	35.8	38.1
2025	7	15	18	23.21	2.42	37.8	0
2025	7	15	19	22.26	2.54	36.5	0
2025	7	15	20	21.33	2.58	34.7	0
2025	7	15	21	20.41	2.5	30.6	0
2025	7	15	22	19.58	2.32	22	0
2025	7	15	23	18.93	2.19	15.6	0

An illustrative one-hour calculation can be shown for 13:00, when the ambient temperature was 28.47 °C, the wind speed was 3.34 m/s, the wind direction was 22.5°, and the global solar radiation was 607.97 W/m². Using the same ACSR 240/40 mm² conductor parameters for both existing lines with $T_{c,max}$ = 75 °C, D = 21.4 mm, ε = 0.5, α = 0.5 and R(75 °C) = 0.14 Ω/km, the implemented IEEE 738 balance gives approximately q_c = 124.7 W/m, q_r = 12.23 W/m and q_s = 6.51 W/m. Accordingly, the allowable current becomes about I_{DLR} = 965.2 A, representing the ampacity of one three-phase 110 kV transmission circuit under the specified meteorological conditions, which corresponds to an approximate transferable power of 183.9 MW at 110 kV for one circuit. This worked example is consistent with the high mid-day DLR values reported in the paper and clearly shows why the DLR case can absorb the efficiency-driven increase in PV output with little or no curtailment on the constrained corridor.

The calculated SLR for the conductor under conservative reference weather is 117.2 MW. In contrast, the DLR profile for 15 July ranges from 171.05 MW to 216.20 MW. When the existing line load is combined with the hourly PV production profile, the peak total export becomes 115.03 MW for Line A and 154.62 MW for Line B. This means that the real thermal margin available on that day is above the conservative static assumption. For Line A, the total export remains below both SLR and DLR throughout the day. For Line B, the midday combination of existing loading and PV production slightly exceeds the static limit, while remaining well below the dynamic limit. This is exactly the type of case where DLR becomes valuable: the additional renewable power exists, but the static operating rule creates avoidable curtailment.

Figure 9 presents the graphical results of the PV plant integration into the existing Line A, together with the corresponding Static Line Rating (SLR) and Dynamic Line Rating (DLR) results. Similarly, Figure 10 presents the results of the PV plant integration into Line B and the corresponding SLR and DLR profiles. The presented DLR results are based on a single representative summer day and should therefore be interpreted as a case-specific assessment rather than a full-year performance evaluation.

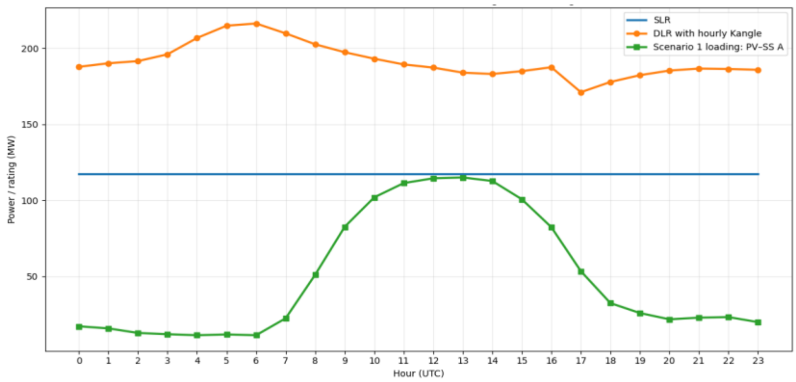

Figure 9. Hourly exportability assessment for Line A.

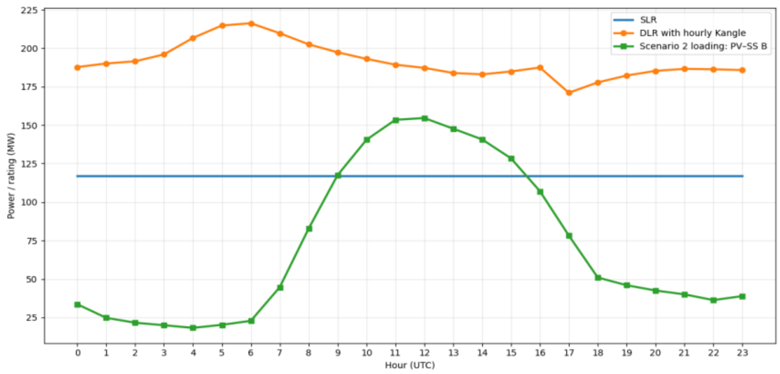

Figure 10. Hourly exportability assessment for Line B.

CONCLUSIONS

This paper integrated two perspectives that are often separated in the literature: production-side efficiency improvement and transmission-side capacity enhancement. In Scenario 1, better PV modules and inverters increased annual energy yield, reduced land demand and improved CO_2 mitigation. The best case was obtained with Jinko Solar modules and a 98% inverter, delivering 118,577 MWh/yr, 128,986 t CO_2/yr of avoided emissions and the smallest land requirement among the analysed options.

In Scenario 2, the hourly thermal capability of a representative ACSR 240/40 mm² 110 kV line was evaluated through SLR and DLR. The calculated SLR was 117.2 MW, while the DLR on the analysed representative summer day ranged from approximately 171.05 MW to 216.2 MW. When the predicted PV output was added to the existing line loading, the Line A corridor remained feasible under both SLR and DLR. In contrast, the Line B corridor experienced transmission constraints under SLR, while DLR significantly increased the available transfer capability and reduced these constraints, although it did not completely eliminate them under peak loading conditions. The presented results are limited to the analysed representative summer day and should not be interpreted as annual DLR performance indicators.

The presented results are limited to the analysed representative summer day and should not be interpreted as annual DLR performance indicators. In addition, the loading profiles represent conservative same-direction thermal screening scenarios based on pre-connection line flows and simulated PV production. They do not represent a complete post-connection AC load-flow study. Therefore, the exact power-flow distribution in the meshed 110 kV network, voltage-rise effects, reactive power requirements, *N*-1 contingency performance, and protection coordination should be assessed in future grid connection studies.

The main message of the study is that the technical value of improved PV conversion efficiency is system-dependent. Production can be increased at plant level, but its full benefit is obtained only when the network can absorb the added output. For the analysed transmission corridors and the representative summer day considered in this study, the results indicate that future renewable integration studies should jointly evaluate module efficiency, inverter efficiency and transmission transfer capability instead of analysing them in isolation.

NASA POWER hourly meteorological data were used because complete hour-by-hour measurements of the required parameters, including air temperature, wind speed, wind direction, and solar irradiance, were not available from official measurement sources in Kosovo for the analysed location and period. Therefore, the results should be interpreted as a representative thermal screening assessment rather than as an operational DLR study based on local field measurements.

FUTURE WORK

Future work should extend the present analysis in four directions. First, the exact azimuth and span-specific meteorological exposure of the analysed transmission lines should be included so that wind-angle effects can be represented more accurately. Second, the DLR assessment should be repeated for a longer time horizon, ideally a full year, in order to quantify seasonal statistics and not only one critical summer day. Third, the daily curtailment analysis should be connected with market prices and avoided reinforcement costs so that the operational and economic benefit of DLR can be expressed in monetary terms. Finally, the same integrated framework can be expanded toward N-1 security analysis, storage support and probabilistic PV forecasting, which would make the study even more relevant for real TSO planning.

NOMENCLATURE

Symbols

A	land area	[m²]
D	conductor diameter	[m]
E	energy	MWh or kWh
I	current	[A]
P	power	[MW] or [kW]
q_c	convective heat loss	[W/m]
q_j	Joule heating	[W/m]
q_r	radiative heat loss	[W/m]
q_s	solar heat gain	[W/m]
Q_{se}	global solar radiation	[W/m²]
$R(T_c)$	conductor resistance at conductor temperature T_c	[Ω/m]
T_a	ambient temperature	[°C]
T_c	conductor temperature	[°C]
VLL	line-to-line voltage	[kV] or [V]
V	wind speed	[m/s]

Greek letters

α	solar absorptivity	[-]
ε	emissivity	[-]

REFERENCES

1. International Renewable Energy Agency (IRENA), Global Energy Transformation: A Roadmap to 2050, International Renewable Energy Agency, Abu Dhabi, United Arab Emirates, 2018, https://www.irena.org/publications/2018/Apr/Global-Energy-Transition-A-Roadmap-to-2050, [Accessed: Jun. 12, 2026].
2. Yang, B., Guo, Z., Wang, J., Duan, C., Ren, Y. and Chen, Y., Key Optimization Issues for Renewable Energy Systems under Carbon-Peaking and Carbon Neutrality Targets: Current States and Perspectives, *Energy Engineering*, Vol. 119, No. 5, pp 1789-1795, 2022, https://doi.org/10.32604/ee.2022.022217.
3. Veeranjaneyulu, I. V., Tripathi, A. K., Pavan, J., Chaitanya, S. and Prasad, C. V. S. R., Design and Implementation of a High-Efficiency 15-Level Asymmetrical Multilevel Inverter for Renewable Energy Applications, E3S Web of Conferences, Vol. 616, 01005, 2025, https://doi.org/10.1051/e3sconf/202561601005.
4. Rana, M., Analysis of Multilevel Inverters in High-Power Applications: The Transformative Role of Power Electronics, *International Journal of Trend in Scientific Research and Development*, Vol. 9, No. 2, pp 464-472, 2025, https://www.ijtsrd.com/papers/ijtsrd78358.pdf, [Accessed: Jun. 12, 2026].
5. Trubitsyn, A., Pierquet, B. J., Hayman, A. K., Gamache, G. E., Sullivan, C. R. and Perreault, D. J., High-Efficiency Inverter for Photovoltaic Applications, *Proceedings of the 2010 IEEE Energy Conversion Congress and Exposition* (ECCE), Atlanta, Georgia, USA, pp 2803-2810, 2010, https://doi.org/10.1109/ECCE.2010.5618163.
6. Shalwar, P. K., Gupta, B., Bhalavi, J. and Bisen, A., Performance Characteristics and Efficiency Enhancement Techniques of Solar PV System: A Review, *F1000Research*, Vol. 11, 1264, 2022, https://doi.org/10.12688/f1000research.126942.1.
7. Saleem, A., Mehmood, K. and Rashid, F., The Efficiency of Solar PV System, *Proceedings of the 2nd International Multi-Disciplinary Conference*, Gujrat, Pakistan, December 19-20, 2016.
8. Jäger-Waldau, A., Kougias, I., Taylor, N. and Thiel, C., How Photovoltaics Can Contribute to GHG Emission Reductions of 55% in the EU by 2030, *Renewable and Sustainable Energy Reviews*, Vol. 126, 2020, https://doi.org/10.1016/j.rser.2020.109836.
9. Rajput, S. K. and Singh, O., Reduction in CO2 Emission through Photovoltaic System: A Case Study, *3rd IEEE International Conference on Nanotechnology for Instrumentation and Measurement*, Guatam Buddha University, Greater Noida, India, 2017, https://www.researchgate.net/publication/327832806, [Accessed: Jun. 12, 2026].
10. Kim, M., Drury, S., Altermatt, P., *et al.*, Identifying Methods to Reduce Emission Intensity of Centralised Photovoltaic Deployment for Net Zero by 2050: Life Cycle Assessment Case Study of a 30 MW PV Plant, *Prog Photovolt Res Appl*, Vol. 31, No. 12, pp 1493-1502, 2023, https://doi.org/10.1002/pip.3747.
11. Deng, Y., Wu, J., Yang, Q., Chen, W., Li, P., Huang, C., Deng, J., Ji, B. and Xie, L., Life Cycle-Based Carbon Emission Reduction Benefit Assessment of Centralized Photovoltaic Power Plants in China, *Sustainability*, Vol. 15, No. 23, 16323, 2023, https://doi.org/10.3390/su152316323.
12. Bolinger, M. and Bolinger, G., Land Requirements for Utility-Scale PV: An Empirical Update on Power and Energy Density, *IEEE Journal of Photovoltaics*, Vol. 12, No. 2, pp 589-594, 2022, https://doi.org/10.1109/JPHOTOV.2021.3136805.

13. Sukumaran, S., Sudhakar, K., Yusop, A. F., Kirpichnikova, I. and Cuce, E., Solar Farm: Siting, Design and Land Footprint Analysis, *International Journal of Low-Carbon Technologies*, Vol. 17, pp 1478-1491, 2022, https://doi.org/10.1093/ijlct/ctac107.
14. van de Ven, D. J., Capellan-Peréz, I., Arto, I., *et al*., The Potential Land Requirements and Related Land Use Change Emissions of Solar Energy, *Scientific Reports*, Vol. 11, No. 1, 2907, 2021, https://doi.org/10.1038/s41598-021-82042-5.
15. Karimi, S., Musilek, P. and Knight, A. M., Dynamic Thermal Rating of Transmission Lines: A Review, *Renewable and Sustainable Energy Reviews*, Vol. 91, pp 600-612, 2018, https://doi.org/10.1016/j.rser.2018.04.001.
16. Institute of Electrical and Electronics Engineers (IEEE), IEEE Standard for Calculating the Current-Temperature Relationship of Bare Overhead Conductors, *IEEE Std 738-2023, Institute of Electrical and Electronics Engineers*, New York, USA, Dec. 2023, https://doi.org/10.1109/IEEESTD.2023.10382442.
17. Martinez, R., Manana, M., Arroyo, A., Bustamante, S., Laso, A., Castro, P. and Minguez, R., Dynamic Rating Management of Overhead Transmission Lines Operating under Multiple Weather Conditions, *Energies*, Vol. 14, No. 4, 1136, 2021, https://doi.org/10.3390/en14041136.
18. Phillips, T., DeLeon, R. and Senocak, I., Dynamic Rating of Overhead Transmission Lines over Complex Terrain Using a Large-Eddy Simulation Paradigm, *Renewable Energy*, Vol. 108, pp 380-389, 2017, https://doi.org/10.1016/j.renene.2017.02.072.
19. Feldhaus, L. and Milek, J., Kosovo's Energy Sector: In Need of a Fresh Start, German Economic Team Newsletter Kosovo, No. 3, Berlin Economics, Berlin, Germany, January-February 2022, https://www.german-economic-team.com/en/newsletter/kosovos-energy-sector-in-need-of-a-fresh-start/, [Accessed: Jun. 12, 2026].
20. Government of the Republic of Kosovo, Energy Strategy of the Republic of Kosovo 2022-2031, Ministry of Economy, Prishtina, Kosovo, 2023, https://me.rks-gov.net/wp-content/uploads/2023/04/Energy-Strategy-of-the-Republic-of-Kosovo-2022-2031-1-1.pdf, [Accessed: Jun. 12, 2026].
21. Zhang, Q., Zhai, Z., Mao, M., Wang, S., Sun, S., Mei, D. and Hu, Q., Control and Intelligent Optimization of a Photovoltaic (PV) Inverter System: A Review, *Energies*, Vol. 17, No. 7, 1571, 2024, https://doi.org/10.3390/en17071571.
22. Lim, S. C., Kim, B. G. and Kim, J. C., Analysis of Inverter Efficiency Using Photovoltaic Power Generation Element Parameters, *Sensors*, Vol. 24, No. 19, 6390, 2024, https://doi.org/10.3390/s24196390.
23. Bahloul, M. and Khadem, S., A Refined Method for Optimising Inverter Loading Ratio in Utility-Scale Photovoltaic Power Plant, *Energy Reports*, Vol. 12, pp 5110-5115, 2024, https://doi.org/10.1016/j.egyr.2024.10.055.
24. Ali, A. O., Elgohr, A. T., El-Mahdy, M. H., *et al*., Advancements in Photovoltaic Technology: A Comprehensive Review of Recent Advances and Future Prospects, *Energy Convers. Manag.: X*, Vol. 26, 2025, https://doi.org/10.1016/j.ecmx.2025.100952.
25. Iturralde Carrera, L. A., Alfonso-Francia, G., Constantino-Robles, *et al*., J., Advances and Optimization Trends in Photovoltaic Systems: A Systematic Review, *Artificial Intelligence*, Vol. 6, No. 9, 225, 2025, https://doi.org/10.3390/ai6090225.
26. Sun, Y., Liu, Y., Wang, B., Lu, Y., Fan, R., Song, X., Jiang, Y., She, X., Shi, S., Ma, K., Zhang, G. and Shen, X., Dynamic Prediction of Overhead Transmission Line Ampacity Based on the BP Neural Network Using Bayesian Optimization, *Frontiers in Energy Research*, Vol. 12, 1449586, 2024, https://doi.org/10.3389/fenrg.2024.1449586.
27. International Council on Large Electric Systems (CIGRE), Guide for Thermal Rating Calculations of Overhead Lines, Technical Brochure 601, Working Group B2.43, CIGRE, Paris, France, 2014.
28. Michiorri, A., Nguyen, H. M., Alessandrini, S., Bremnes, J. B., Dierer, S., Ferrero, E., Nygaard, B. E., Pinson, P., Thomaidis, N. and Uski, S., Forecasting for Dynamic Line

Rating, *Renewable and Sustainable Energy Reviews*, Vol. 52, pp 1713-1730, 2015, https://doi.org/10.1016/j.rser.2015.07.134.

29. Douglass, D. A. and Edris, A.-A., Field Studies of Dynamic Thermal Rating Methods for Overhead Lines, *Proceedings of the 1999 IEEE Transmission and Distribution Conference*, New Orleans, Louisiana, USA, Vol. 2, pp 842-851, 1999, https://doi.org/10.1109/TDC.1999.756160.
30. Black, C. R. and Chisholm, W. A., Key Considerations for the Selection of Dynamic Thermal Line Rating Systems, *IEEE Transactions on Power Delivery*, Vol. 30, No. 5, pp 2154-2162, 2015, https://doi.org/10.1109/TPWRD.2014.2376275.
31. Seppa, T. O., Increasing Transmission Capacity by Real-Time Monitoring, *Proceedings of the 2002 IEEE Power Engineering Society Winter Meeting*, New York, New York, USA, Vol. 2, pp 1208-1211, January 27-31, 2002, https://doi.org/10.1109/PESW.2002.985201.
32. Natural Resources Canada, RETScreen Software Online User Manual: Small Hydro Project Model, Natural Resources Canada, Ottawa, Ontario, Canada, 2004, http://www.retscreen.net, [Accessed: Jun. 12, 2026].
33. Natural Resources Canada, Clean Energy Project Analysis: RETScreen Engineering & Cases Textbook, 3rd ed., Minister of Natural Resources Canada, Ottawa, Ontario, Canada, 2005, https://publications.gc.ca/site/eng/9.690261/publication.html, [Accessed: Jun. 12, 2026].
34. Kosovo Transmission System, Market and System Operator (KOSTT), Transmission Development Plan 2026-2035, Kosovo Transmission System, Market and System Operator, Prishtina, Kosovo, 2025, https://kostt.com/Content/ViewFiles/Index/plani10viteEN.pdf, [Accessed: Aug. 25, 2026].
35. Energy Regulatory Office (ERO), Annual Report 2025, Energy Regulatory Office, Prishtina, Kosovo, 2026, https://www.ero-ks.org/zrre/sites/default/files/Publikimet/Raportet%20Vjetor/Raporti%20vjetor%202025.pdf, [Accessed: Jun. 12, 2026].

Paper submitted: 18.03.2026
Paper revised: 30.06.2026
Paper accepted: 19.07.2026